

Document downloaded from:

<http://hdl.handle.net/10251/180305>

This paper must be cited as:

Jimenez, N.; Ealo, J.; Muelas-Hurtado, R.; Duclos, A.; Romero-García, V. (2021). Sub-Diffractive Acoustic Vortices by Nonlinear Mixing. IEEE. 1-4.
<http://hdl.handle.net/10251/180305>



The final publication is available at

<https://doi.org/10.1109/IUS52206.2021>

Copyright IEEE

Additional Information

Sub-diffractive acoustic vortices by nonlinear mixing

Noé Jiménez*, Joao Ealo†, Rubén Muelas-Hurtado†, Aroune Duclos‡ and Vicent Romero-García‡

*Instituto de Instrumentación para Imagen Molecular, Universitat Politècnica de València, Spain

Email: nojigon@upv.es

†School of Mechanical Engineering, Universidad del Valle, Cali, Colombia

‡Laboratoire d'Acoustique de l'Université du Mans, CNRS, Le Mans Université, Le Mans, France

Abstract—Vortex beams, characterized by a collimated wavefront with a phase dislocation at their principal axis, have found practical applications to construct acoustic tweezers for particle trapping and manipulation, or underwater communications. However, the natural diffraction of the wavefront limits the size of the vortex. This result in vortices whose bright core is larger than the wavelength, limiting their use for practical applications such as long-range underwater communications. In this work, we synthesize a vortex beam of sub-wavelength size at a distance beyond Rayleigh diffraction length using the nonlinear mixing of two confocal, high-frequency and detuned vortex beams of different topological charges. By using the nonlinear mixing of two confocal vortices, it was generated a low-frequency (1 kHz) focused vortex beam of integer topological charge whose distance between magnitude maxima is about 18 times smaller than its wavelength at a distance about 3 times the Rayleigh diffraction length. Sub-wavelength vortices emerge as a result of the spatiotemporal interference of two primary vortex beams due to the conservation of angular momentum during nonlinear wave-mixing. This mechanism opens new paths to design directive parametric antennas for vortex transceivers or particle manipulation systems at scales well below the diffraction limit.

Index Terms—Acoustic vortices, nonlinear acoustics, ultrasound, sub-diffractive propagation, sub-wavelength limit.

I. INTRODUCTION

Vortex beams are characterized by a collimated wavefront with a phase dependence of the type $\exp(il\phi)$, with ϕ the azimuthal angle and l the topological charge, respectively. At the principal axis of the vortex beam the field exhibits a phase singularity and the field is null. Methods to synthesize these beams include active devices such as phased arrays [1], helical radiating surfaces [2] or Archimedean [3], [4], Fresnel spiral diffraction gratings [5], or acoustic holograms [6], among others. Metamaterials have also been used to generate vortex beams by using flat and sub-wavelength structures [7], [8]. However, in all these configurations the natural diffraction of the wavefront limits the size of the vortex. The minimum value is only reached for distances smaller than the Rayleigh

We acknowledge financial support from the Spanish Ministry of Science, Innovation and Universities through grant “Juan de la Cierva – Incorporación” (IJC2018-037897-I) and PID2019-111436RB-C22, and by the Agència Valenciana de la Innovació through grants INIVAL10/19/016. This article is based upon work from COST Action DENORMS CA15125. JPG and VRG gratefully acknowledge projects ANR-RGC METARoom (ANR-18-CE08-0021) and the HYPERMETA funded under the program Étoiles Montantes of the Région Pays de la Loire.

diffraction length of the source due to the divergence of the beam, given by the relation between the geometry of the source and the wavelength. Recently, increasing attention has been paid to restoring the evanescent components of a field to overcome the diffraction limit either using metamaterials [9] or time-reversal techniques [10]. However, as these approaches rely on evanescent waves, their use is restricted to near-field distances.

In this work [11], we synthesize a vortex beam of sub-wavelength size at a distance beyond Rayleigh diffraction length using the nonlinear mixing of two confocal, high-frequency and detuned vortex beams of different topological charges. We demonstrate the concept using the natural self-demodulation phenomenon in air. We generate a focused vortex beam of integer topological charge whose distance between magnitude maxima is about 18 times smaller than its wavelength at a distance about 2.8 times the Rayleigh diffraction length.

II. METHODS

A device was manufactured by disposing 10-mm diameter ultrasound emitters operating in air over two different helical surfaces as shown in Fig. 1. The helical profile of the n -th surface (with $n = 1, 2$) was designed to generate a focused beam at a focal point, $\mathbf{r}(\phi, r, z) = (0, 0, F)$, and, simultaneously, produce at this location a difference of time of flight equal to $\Delta t_n = l_n \phi / \omega_n$, where l_n is the topological charge of the n -th primary vortex beam, ω_n the angular frequency and ϕ the azimuthal coordinate. In particular, the first source, composed of the two internal concentric rings of transducers, see Fig. 1 (b), was excited with a sinusoidal pulse burst of $\omega_1/2\pi = 40$ kHz while the second one, composed of the two external concentric rings of transducers, was excited at $\omega_2/2\pi = 41$ kHz. The topological charges of the primary vortex beams, defined by the curvature of the helical surfaces, were set to $l_1 = 1$ and $l_2 = 2$. Source aperture was set to $2a = 110$ mm, with a the radius of the source, and the focal point was $F = 100$ mm. Thus, the Rayleigh distances for the primary vortex beams are around $\pi a^2 / \lambda_1 \approx \pi a^2 / \lambda_2 \approx 1.1$ m.

The generation of the two confocal primary vortex beams is based on a helical surface. The surface should produce the focusing of the acoustic waves at the focal point $\mathbf{r}(x, y, z) = \mathbf{r}(0, 0, F)$ and, simultaneously, a phase dislocation at this

point. The time-of-flight at the focal spot should present an azimuthal dependence of the type

$$\Delta t_n(\phi) = \frac{l_n \phi}{\omega_n}, \quad (1)$$

where l_n is the topological charge and ω_n the angular frequency of the n -th vortex beam and the azimuthal angle. To guarantee such phase, we design a helical surface as shown in Fig. 1. The surface design is constrained by the distance to the focal point, which must follow this relation

$$R_n(\phi) = F - \frac{l_n \lambda_n \phi}{2\pi}, \quad (2)$$

at any point, where $\lambda_n = 2\pi c_0/\omega_n$. This surface, defined in spherical coordinates as $\mathbf{r} = \mathbf{r}(\phi, \theta, R_n(\phi))$, can be expressed in Cartesian coordinates as

$$x_n(\phi, \theta) = R_n(\phi) \cos(\phi) \sin(\theta), \quad (3)$$

$$y_n(\phi, \theta) = R_n(\phi) \sin(\phi) \sin(\theta), \quad (4)$$

$$z_n(\phi, \theta) = -[F + R_n(\phi) \cos(\theta)], \quad (5)$$

where the azimuthal and elevation angles range between $0 < \phi < 2\pi$ and $\theta_{\min}^{[n]} < \theta < \theta_{\max}^{[n]}$, respectively. The aperture angles are given by

$$\theta_{\max}^{[2]} = \tan^{-1}\left(\frac{a}{2F}\right), \quad (6)$$

$$\theta_{\min}^{[2]} = \tan^{-1}\left(\frac{a_h}{2F}\right), \quad (7)$$

$$\theta_{\max}^{[1]} = \theta_{\min}^{[2]}, \quad (8)$$

$$\theta_{\min}^{[1]} = 0, \quad (9)$$

where $2a$ is the outer-source aperture and $2a_h$ is the aperture of the inner source.

The two vortex sources were manufactured by placing two concentric arrays of transducers over the helical surfaces. Each

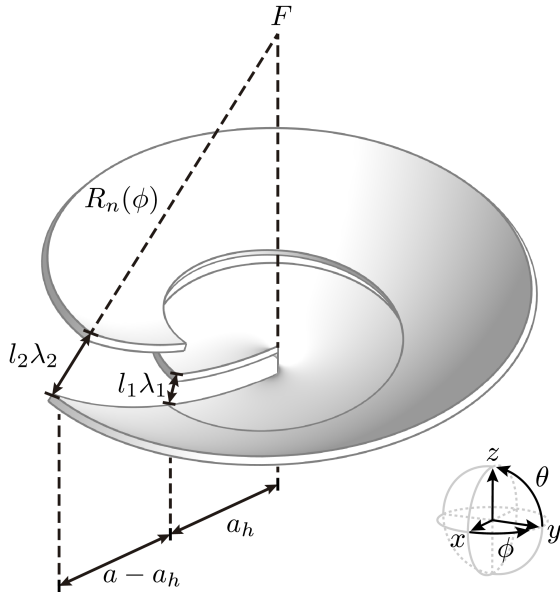


Fig. 1. Scheme of the helical surface to focus two confocal vortex beams.

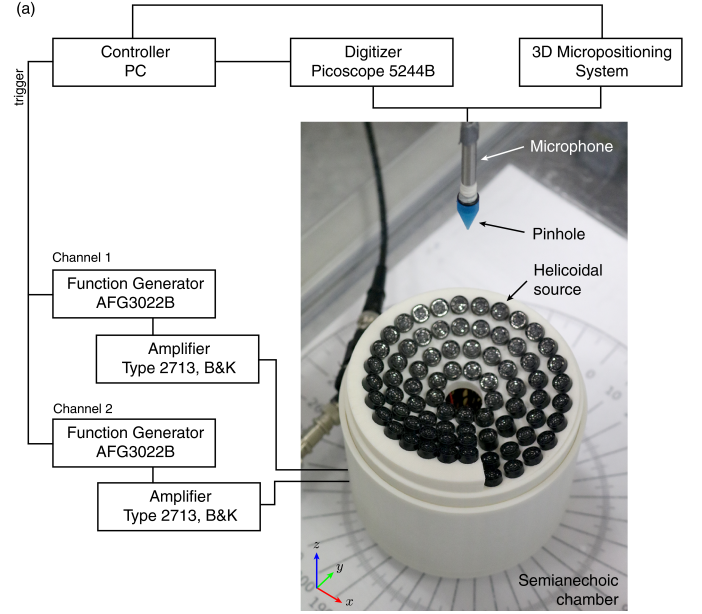


Fig. 2. Experimental setup.

of the sources was composed of two concentric arrays of piezoelectric transducers, as shown in Fig. 2. Each piezoelectric transducer (MA40S4S, Murata Manufacturing Co., Ltd.) presents an aperture of 10 mm and produces a sound pressure level of 120 dB SPL (0 dB = 20 μ Pa) measured at 30 cm in air when excited with a sinusoidal signal of 10 V. The source consisted in a total of 74 transducers (50 for the inner and 24 for the outer source). Transducers were connected in parallel. For the first source (inner array) the design frequency was $f_1 = 40$ kHz while for the second one (outer array) the frequency was $f_2 = 41$ kHz. The topological charges of the primary vortex beams were set to $l_1 = 1$ and $l_2 = 2$. Source aperture was $2a = 110$ mm ($2a_h = 60$ mm) and the focal was $F = 100$ mm.

III. RESULTS

For finite-amplitude waves, and when all emitters are active, both beams interact and due to material and advective nonlinearity wave mixing occurs during propagation. Higher harmonics arise as arithmetical combinations of the fundamental waves of both beams. The root-mean-square pressure measured was 138.4 Pa at 40 kHz (a sound pressure level of 136.8 dB referenced at 20 μ Pa), enough to trigger weak nonlinear effects. In addition to higher harmonics, a difference-frequency mode of frequency $\omega_d = \omega_2 - \omega_1$ was generated due to the nonlinear self-demodulation of the beating wavefront.

As homogeneous acoustic media lack of strong dispersion, phase-matching holds during nonlinear propagation and harmonic generation processes are cumulative with distance. On the one hand, it is expected that the locally generated self-demodulated mode presents a field spatial distribution similar to those of the primary beams, as occurs in parametric acoustic antennas [12]. On the other hand, the phase of the self-

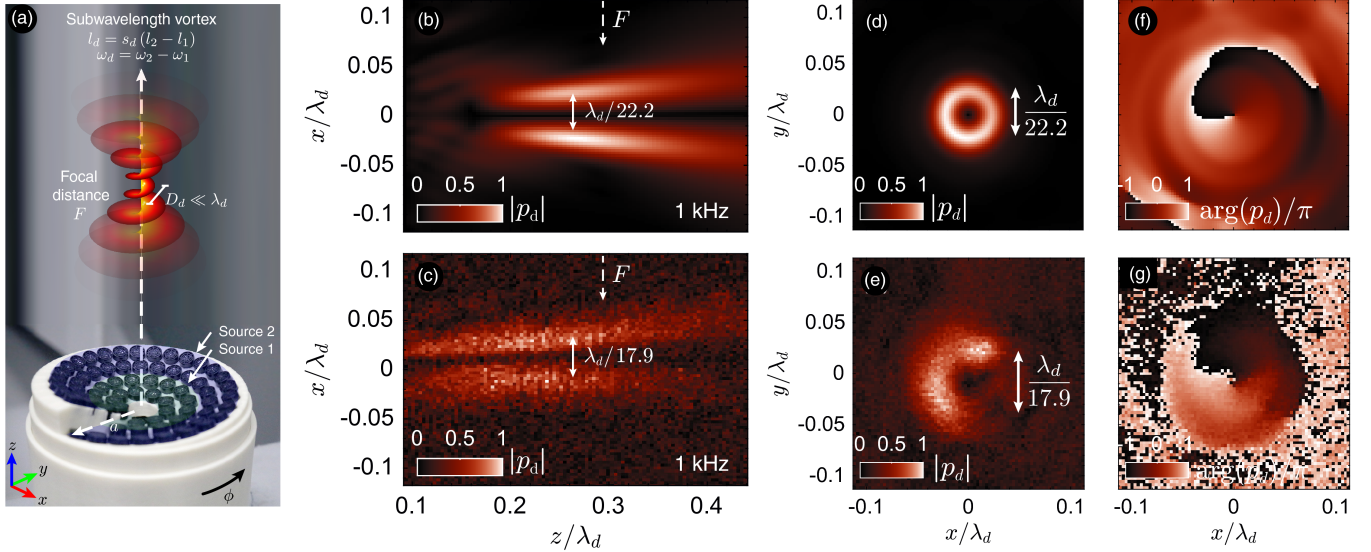


Fig. 3. (a) scheme of the self-demodulated field. (b) and (c) show the sagittal field cross-sections at $y = 0$ showing the theoretical and measured demodulated component, respectively. (d-e) Transverse field cross-section at $z = 80$ mm showing the normalized magnitude and the normalized phase of the theoretical and measured demodulated component, respectively. (g) Normalized field magnitude cross-section at 1 kHz obtained experimentally, numerically and by linear theory. Input: Phase of the self-demodulated field along the azimuthal coordinate.

demodulated beam depends on the spatiotemporal interference of the two vortex beams, which is linked to their topological charges. This results in a self-demodulated beam with a phase factor $\exp(il_d\phi)$ where the topological charge of the self-demodulated beam is

$$l_d = s_d(l_2 - l_1), \quad (10)$$

where $s_d = \text{sign}(\omega_2 - \omega_1)$, due to the conservation of topological charge of nonlinear vortices, which is indeed a consequence of the conservation of angular momentum [13]. Particular attention should be paid to Eq. (10) because this is not valid if the frequencies of the primary beams are commensurable [14]. However, in self-demodulation applications, this is usually fulfilled as the primary beams are commonly chosen with nearby frequencies. Therefore, to synthesize a sub-wavelength vortex by self-demodulation, the primary beams should present different topological charges and frequencies, and, in addition, their field distribution must overlap in space. Simulated and experimental results are shown in Figs. 3. A low-frequency beam at $\omega_d = 1$ kHz is generated locally, and its spatial distribution matches the overlapping volume of the two primary beams. Its corresponding wavelength is $\lambda_d = 2\pi c_0/\omega_d \gg \lambda_n$, therefore, the width of the beam, dominated by the width of the primary beams, is deep sub-wavelength.

The self-demodulated vortex arises as a result of the nonlinear mixing of the two primary vortex beams. Its topological charge is given by $l_d = l_2 - l_1 = 1$, showing the conservation of topological charge and, therefore, the conservation of orbital angular momentum during the nonlinear mixing of the primary beams as given by Eq. (10). The transversal pressure-field distribution of the self-demodulated vortex beam at $z = 80$

mm and $y = 0$ mm. The width of the vortex, D_d , is 17.9 times smaller than the wavelength in the experimental observations ($D_d = \lambda_d/22.2$ in simulations). Note that the measurement distance is 2.8 times the Rayleigh diffraction length for the self-demodulated mode. The field at the axis ($x = 0$) becomes null due to the phase singularity. The phase of the beam along the azimuthal coordinate ϕ , depicted in Fig. 4, agrees with a linear profile of $(l_2 - l_1)\phi = l_d\phi$, demonstrating the topological charge conservation during nonlinear mixing. Using this approach, vortices of arbitrary topological charge and size can be synthesized by tuning the parameters of the primary beams.

IV. CONCLUSIONS

In this work we have shown the sub-wavelength and sub-diffractive generation of acoustic vortices at distances beyond Rayleigh diffraction length by using the nonlinear self-

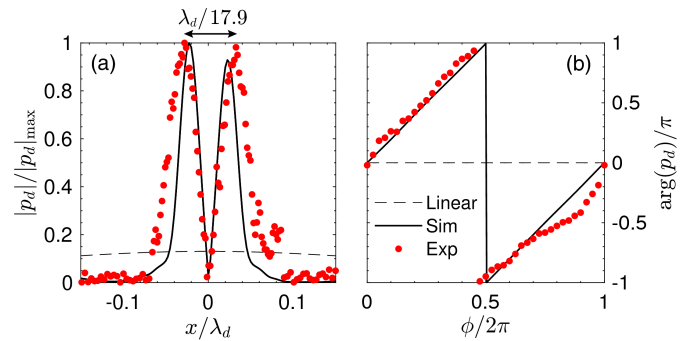


Fig. 4. (a) Normalized field magnitude cross-section at 1 kHz obtained experimentally, numerically and by linear theory. (b) Phase of the self-demodulated field along the azimuthal coordinate.

demodulation. Sub-wavelength vortices emerge because of the spatiotemporal interference of two primary vortex beams due to the conservation of angular momentum during nonlinear wave-mixing.

REFERENCES

- [1] B. T. Hefner and P. L. Marston, "An acoustical helicoidal wave transducer with applications for the alignment of ultrasonic and underwater systems," *Jour. Acous. Soc. Am.*, vol. 106, no. 6, pp. 3313–3316, 1999.
- [2] J. L. Ealo, J. C. Prieto, and F. Seco, "Airborne ultrasonic vortex generation using flexible ferroelectrets," *IEEE Trans. Ultrason. Ferroelectr. Freq. Control*, vol. 58, no. 8, pp. 1651–1657, 2011.
- [3] N. Jiménez, V. Sánchez-Morcillo, R. Picó, L. García-Raffi, V. Romero-García, and K. Staliunas, "High-order acoustic Bessel beam generation by spiral gratings," *Physics Procedia*, vol. 70, pp. 245–248, 2015.
- [4] N. Jiménez, R. Picó, V. Sánchez-Morcillo, V. Romero-García, L. M. García-Raffi, and K. Staliunas, "Formation of high-order acoustic Bessel beams by spiral diffraction gratings," *Phys. Rev. E*, vol. 94, no. 5, p. 053004, 2016.
- [5] N. Jiménez, V. Romero-García, L. M. García-Raffi, F. Camarena, and K. Staliunas, "Sharp acoustic vortex focusing by Fresnel-spiral zone plates," *Appl. Phys. Lett.*, vol. 112, no. 20, p. 204101, 2018.
- [6] S. Jiménez-Gambín, N. Jiménez, and F. Camarena, "Transcranial focusing of ultrasonic vortices by acoustic holograms," *Physical Review Applied*, vol. 14, no. 5, p. 054070, 2020.
- [7] A. Marzo, A. Ghobrial, L. Cox, M. Caleap, A. Croxford, and B. Drinkwater, "Realization of compact tractor beams using acoustic delay-lines," *Appl. Phys. Lett.*, vol. 110, no. 1, p. 014102, 2017.
- [8] X. Jiang, Y. Li, B. Liang, J.-c. Cheng, and L. Zhang, "Convert acoustic resonances to orbital angular momentum," *Phys. Rev. Lett.*, vol. 117, no. 3, p. 034301, 2016.
- [9] J. B. Pendry, "Negative refraction makes a perfect lens," *Phys. Rev. Lett.*, vol. 85, no. 18, p. 3966, 2000.
- [10] G. Lerosey, J. De Rosny, A. Tourin, and M. Fink, "Focusing beyond the diffraction limit with far-field time reversal," *Science*, vol. 315, no. 5815, pp. 1120–1122, 2007.
- [11] N. Jiménez, J. Ealo, R. D. Muelas-Hurtado, A. Duclos, and V. Romero-García, "Subwavelength acoustic vortex beams using self-demodulation," *Physical Review Applied*, vol. 15, no. 5, p. 054027, 2021.
- [12] P. J. Westervelt, "Parametric acoustic array," *Jour. Acous. Soc. Am.*, vol. 35, no. 4, pp. 535–537, 1963.
- [13] J.-L. Thomas and R. Marchiano, "Pseudo angular momentum and topological charge conservation for nonlinear acoustical vortices," *Phys. Rev. Lett.*, vol. 91, no. 24, p. 244302, 2003.
- [14] R. Marchiano and J.-L. Thomas, "Doing arithmetic with nonlinear acoustic vortices," *Physical review letters*, vol. 101, no. 6, p. 064301, 2008.